



# Modelling of diffusion from equilibrium diffraction fluctuations in ordered phases

E. Arapaki<sup>b</sup>, P. Argyrakis<sup>b</sup>, M.C. Tringides<sup>a,\*</sup>

<sup>a</sup> Iowa State University, Ames Laboratory-USDOE, Ames, IA 50011, United States

<sup>b</sup> Department of Physics, University of Thessaloniki, 54124 Thessaloniki, Greece

## ARTICLE INFO

### Article history:

Received 11 October 2007

Accepted for publication 14 April 2008

Available online 18 April 2008

### Keywords:

Surface diffusion

Fluctuations

Collective diffusion

Phase transitions

Lattice gas models

Interactions

## ABSTRACT

Measurements of the collective diffusion coefficient  $D_c$  at equilibrium are difficult because they are based on monitoring low amplitude concentration fluctuations generated spontaneously, that are difficult to measure experimentally. A new experimental method has been recently used to measure time-dependent correlation functions from the diffraction intensity fluctuations and was applied to measure thermal step fluctuations. The method has not been applied yet to measure superstructure intensity fluctuations in surface overlayers and to extract  $D_c$ . With Monte Carlo simulations we study equilibrium fluctuations in Ising lattice gas models with nearest neighbour attractive and repulsive interactions. The extracted diffusion coefficients are compared to the ones obtained from equilibrium methods. The new results are in good agreement with the results from the other methods, i.e.,  $D_c$  decreases monotonically with coverage  $\theta$  for attractive interactions and increases monotonically with  $\theta$  for repulsive interactions. Even the absolute value of  $D_c$  agrees well with the results obtained with the probe area method. These results confirm that this diffraction based method is a novel, reliable way to measure  $D_c$  especially within the ordered region of the phase diagram when the superstructure spot has large intensity.

© 2008 Elsevier B.V. All rights reserved.

## 1. Introduction

The thermodynamic analysis of diffusion is based on quantities that are commonly defined under equilibrium conditions in terms of low amplitude long wavelength concentration fluctuations [1–8]. The diffusion coefficient is determined from the inverse of the relaxation time of these concentration fluctuations. A system under equilibrium conditions, with local coverage  $\theta(r, t)$  and average coverage  $\theta_{av}$  can have concentration fluctuations of strength  $\Delta\theta = |\langle\delta\theta^2(0, 0)\rangle|^{1/2}$  which are generated spontaneously or are imposed externally.  $\delta\theta(r, t) = (\theta(r, t) - \theta_{av})$  is the strength of the fluctuation at position  $r$  and time  $t$ . The fluctuation will relax in time and a good measure of the relaxation can be obtained from the autocorrelation function  $S(r' - r, t) = \langle\delta\theta(r, 0)\delta\theta(r', t)\rangle$ .

The averaging can be realized either as a time average or as a spatial average over all sites in the system, since the ergodic property guarantees that the system explores the available phase space equivalently, either in the space or in the time domain. The diffusion equation is linear for systems at equilibrium (even when the collective diffusion coefficient  $D_c(\theta)$  is coverage dependent) and is also obeyed by  $S(r' - r, t)$ .

$$\frac{\partial S(r' - r, t)}{\partial t} = \nabla D_c(\theta) \nabla S(r' - r, t) \approx D_c(\theta) \nabla^2 S(r' - r, t) \quad (1)$$

Truly equilibrium systems have low amplitude concentration fluctuations over the average coverage  $\theta_{av}$ , i.e.,  $|\langle\delta\theta^2(0, 0)\rangle|^{1/2} / \theta_{av} \ll 1$  and therefore a constant diffusion coefficient can be assumed, even at finite coverage. The solution for  $S(r' - r, t)$  is given by

$$S(r' - r, t) = S_0 (\exp -((r' - r)^2 / 4D_c t)) / 4\pi D_c t \quad (2)$$

with  $S_0 = \langle\delta\theta^2(0, 0)\rangle$ . Despite the importance of correlation functions in defining equilibrium diffusion and in relating the dependence of  $D_c$  on  $\theta$ ,  $T$  to the thermodynamic properties of the system, very few experimental techniques have been developed to accomplish this. The extraction of  $D_c$  from Eq. (2) requires the measurement of time correlations between fluctuations at two sites separated by distance  $r' - r$ . Such measurements are difficult in real space because they require precise control of the separation ( $r' - r$ ) and the measurable signal is low if only single sites are probed. This can be overcome if a finite area is used to measure the fluctuations [9]. This method has been implemented successfully in electron tunneling processes by exploiting the high magnification  $\sim 10^6$  of the field emission microscope (FEM) [9] or STM [10,11].  $D_c$  is given by the time constant  $\tau$  of the decay of the autocorrelation function of the fluctuations and the probe area  $A$ ,  $D_c = A/4\tau$ . However, the electron emission process requires high electric fields (typically  $\sim 0.5$  V/Å) which can bias the diffusion towards the tip by “tilting” the potential energy surface [11]. If this is the case the extracted diffusion barrier from these measurements might not be the one for the ideal surface.

\* Corresponding author. Tel.: +1 515 294 6439; fax: +1 515 294 0689.  
E-mail address: [tringides@ameslab.gov](mailto:tringides@ameslab.gov) (M.C. Tringides).

A different implementation of equilibrium diffusion methods is based on measuring the Fourier transforms of  $S(r, t)$ , i.e., either the elastic structure  $S(q, t)$  or the quasi-elastic structure factor  $S(q, \omega)$ . The first method is implemented with optical techniques by imposing a concentration profile variation of fixed wavelength  $\lambda = 2\pi/q$  and measuring the relaxation back to equilibrium in systems of low desorption temperature [12]. However the spatial resolution of the method is several micrometers so it can easily include surface inhomogeneities (steps, defects, etc.). The second method is based on quasi-elastic He-scattering experiments which can measure the full  $q$  and  $\omega$  dependence of the structure factor [13]. Since one spatial Fourier component is present at fixed wavevector  $q$ , the time constant of the decay  $\tau$  or the inverse of the frequency loss  $\tau = (\Delta\omega)^{-1}$  in scattering experiments can be used to deduce the value of the diffusion coefficient  $D_c = (2\pi/q)^2/\tau$ . However rather large values of  $q$  are commonly probed (corresponding to hops to neighbouring sites instead of distant sites) so it is not clear if  $D_c$  can always be extracted in the long wavelength limit  $q \rightarrow 0$  (especially at high coverage in interactive systems).

## 2. Diffraction intensity fluctuations and $D_c$

Despite the use of these methods, there is still need for more widely applicable methods which can be used under all experimental conditions. It has been recently shown that it is possible to use reciprocal space based methods (i.e., surface diffraction) to measure equilibrium fluctuations and monitor time-dependent phenomena [14–17]. In addition to the advantage of the absence of electric fields and small variations in concentration, diffraction based methods are wavevector selective and therefore are sensitive to different regions of the phase diagram. In such methods the equilibrium diffracted intensity is measured as a function of time

$$I(\vec{q}, t) = \frac{1}{(N\Theta)^2} \int \theta(\vec{r}, t) \theta(\vec{r} + \vec{r}, t) \exp(-i\vec{q} \cdot \vec{r}) d\vec{r} d\vec{r}' \quad (3)$$

and can be related to the Fourier transform of the dynamic structure factor  $S(q, t)$  at the wavevector  $q$  of the ordered phase which is being monitored. The fluctuation of  $I(q, t)$  from its average value  $\overline{I(q, t)}$  at time  $t$ , is defined by  $\delta I(q, t) = I(q, t) - \overline{I(q, t)}$ . Although it involves 4-point correlation functions, as shown in Ref. [14], in general it can be written in terms of  $S(q, t)$

$$G(q, t) = \langle \delta I(q, 0) \delta I(q, t) \rangle = pS^2(q, t) \quad (4)$$

with  $p$  a constant which depends on the details of the system under investigation. In [14] the functional form of the correlation function was also derived under the assumption that memory effects play no role. This is the common assumption in most theoretical approaches to the diffusion problem. This assumption is equivalent to statistically independent successive jumps (i.e., Markovian diffusion process). The method has been already applied to measure thermally induced fluctuations on stepped surfaces (W(430) and Si(100)) and the experimental conditions necessary to carry out such experiments have been clarified [14–16]. Although the idea of such diffraction experiments is straightforward it has not been implemented earlier because of demanding experimental requirements: the beam size  $d$  of the scattered probe in a diffraction experiment is larger than the coherence length of the diffractometer  $\xi$  and includes  $M = (d/\xi)^2$  incoherent scattering regions, which reduces the fluctuation signal by  $1/\sqrt{M}$  since they are uncorrelated in space or in time. Highly bright electron sources (i.e., number of electrons per solid angle per time), channeltron-based high resolution diffractometers and long acquisition times in noise-free instruments can overcome this problem and thus enable measurable signal to be extracted. With the LEED diffractometers used so far

in the previous experiments [14–16] the reciprocal space resolution was better than 0.3%BZ (so the coherence length is  $\xi \sim 400$  nm) the acquisition speed was less than 20 ms and collection times were 2–3 h to extract a fluctuation signal that is 5–6 times larger than the statistical noise. These experimental conditions are adequate without reducing the beam size  $d$  because the incident beam brightness (i.e., number of electrons per second per solid angle) provides sufficient counts in sufficiently short measuring time. Such fluctuation measurements have been also pursued in “speckle” X-ray experiments [17], where the incident beam size is reduced to size comparable to the coherence length  $d \sim L$  ( $\mu\text{m}$  size aperture) to avoid the  $1/\sqrt{M}$  intensity reduction.

However, no work has been carried out to test the new method in surface overlayers, to measure concentration fluctuations to extract the collective diffusion coefficient  $D_c$  and to show that it is legitimate and consistent with  $D_c$  extracted with other equilibrium methods. It is the purpose of this work to make such tests in theoretical models with the use of Monte Carlo simulations which can extend the validity of the method and can motivate corresponding experiments in relevant systems. We calculate correlation functions and extract the relaxation time constants for two sets of interactions under equilibrium to deduce the coverage, temperature dependence and effective activation energies for  $D_c$  defined in terms of the decay constants from Eqs. (2) and (3). It is not obvious that they should have similar dependence on  $T$ ,  $\theta$  as the ones extracted from conventional approaches, i.e., the decay of the concentration fluctuations within a probe area (as in the FEM or the STM geometry).

In the current work an Ising model within a lattice gas on a square lattice with short range interactions, either repulsive or attractive, is used although similar analysis can be carried out on any system with other types of interactions and with any symmetry of the order parameter. Repulsive interactions result in  $c(2 \times 2)$  domains for temperatures below the critical temperature  $J/kT_c > 1.76$  (for  $\theta = 0.5$ ) at the ordering wavevector  $q = (\pi/a, \pi/a)$ . Since the unit vectors of the  $c(2 \times 2)$  sublattice are  $a(\hat{x} + \hat{y})/\sqrt{2}$  and  $a(\hat{x} - \hat{y})/\sqrt{2}$  (with  $\hat{x}, \hat{y}$  the unit vectors along the axes of the square lattice), the  $(\pi/a, \pi/a)$  wavevector measures long range order in the system and correctly probes the relaxation of long wavelength fluctuations. For attractive interactions there is coexistence between regions of high concentration (i.e.,  $(1 \times 1)$  islands with  $\theta = 1$  ML) and empty regions (with  $\theta = 0$  ML). Depending on the size of the  $(1 \times 1)$  domains a characteristic wavevector  $q_{\text{max}}$  is seen where  $S(q)$  has a maximum, which shifts towards zero, as the average domain size  $1/q_{\text{max}}$  becomes larger.

As will be seen in Section 5 the agreement between the probe area [18] and the diffraction based methods is good. This quantitative analysis of the correlation functions in the simulations and the comparison with previous results can be used as evidence for extending such diffraction fluctuation experiments to measure  $D_c$ . The analysis can be applicable in other more complicated models. It can be also of value when information about the interaction parameters is unknown. The fit of the shape and decay constants of the experimentally measured vs simulated correlation functions can be used as a guide to deduce the interaction parameters.

These recent experimental capabilities also raise theoretical questions since it is important in a system with a given set of interactions to estimate both the fluctuation strength  $\langle \Delta S^2(q, 0) \rangle^{1/2}$  and the functional form of the correlation function in time. Both of these quantities will depend on the interaction parameters and the temperature of the system.

In Section 3 we give a brief description of the computer program and the quantities calculated, in Section 4 we present the results obtained for the two types of interactions and compare them with results obtained by the previous probe area methods. In Section 5 we discuss in detail the comparison between diffraction

fluctuation method vs probe area fluctuation method and its significance as a method of measuring  $D_c$ . Finally in the last section we summarize the evidence supporting the diffraction fluctuation method and discuss open questions. Hopefully these initial results will motivate additional experiments/simulations to test further the analysis for broader use by the diffusion community.

### 3. Description of the simulation model

A lattice gas model on a square lattice is used for the modelling. The size of the matrix is  $L \times L$  to simulate the surface area, the number of sites  $N = L^2$  and the number of atoms on the surface  $N\theta$  where  $\theta$  is the coverage. The initial configuration was generated by randomly depositing the  $N\theta$  atoms on the lattice. The nearest neighbour interaction parameter  $J$  is positive for attractive and negative for repulsive interactions. A state of the system defined by the ratio  $J/kT$  (where  $T$  is the temperature and  $k$  is the Boltzmann constant) was generated by discarding the initial Monte Carlo steps (MCSs) to attain equilibrium. A MCS is defined as the number of steps where on average each atom is interrogated once. The flipping algorithm was based on the initial site energy  $E_i = zJ$  where  $z$  is the number of nearest neighbour atoms of the interrogated atom. The probability for the interrogated atom to move to a neighbouring site is given by  $p = e^{-(E_i/kT)}/p_{\max}$  where  $p_{\max} = 1$  for  $J > 0$  (attractive) and  $p_{\max} = e^{-3J/kT}$  for  $J < 0$  (repulsive) interactions. These choices ensure that the hopping probability is always less than one.

### 4. Results

Fig. 1 shows the value of the normalized  $S_{\max}/(N\theta)^2$  vs  $t$  for  $\theta = 0.5$  ML and the case of attractive interactions  $J/kT = 2.2$ . The characteristic wavevector is  $q_{\max} = (\pi/21, \pi/21)$  for  $L = 21$  and  $S_{\max}/(N\theta)^2$  fluctuates around its average value indicating that indeed we have reached equilibrium. About  $10^5$  MCSs have been discarded for this particular temperature necessary to ensure equilibrium. This is the typical number of MCS discarded for attractive interactions. The corresponding number of MCS discarded is  $10^4$  for the case of repulsive interactions because the nature of the phase transition is different, i.e., for attractive interactions there is coexistence between  $(1 \times 1)$  islands and the empty lattice phase, while for repulsive interactions a typical finite temperature

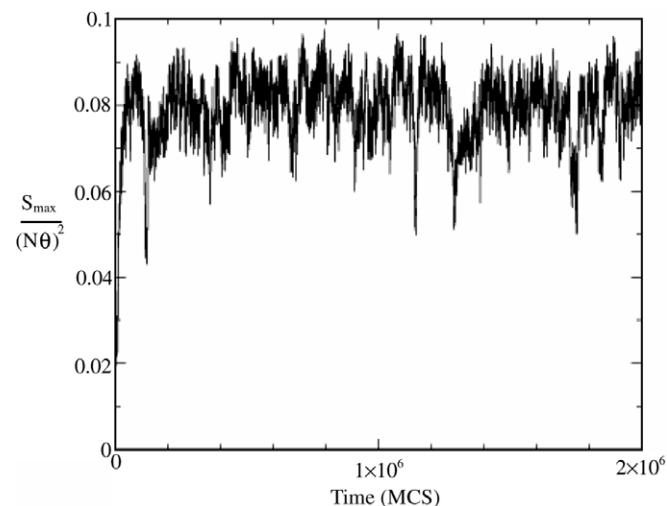


Fig. 1. The normalized  $S_{\max}/(N\theta)^2$  vs  $t$  for  $\theta = 0.5$  ML and the case of attractive interactions  $J/kT = 2.2$  at the characteristic wavevector is  $q_{\max} = (\pi/L, \pi/L)$ . About  $10^5$  MCSs have been discarded to ensure equilibrium.

configuration includes the two equivalent  $c(2 \times 2)$  domains. To ensure that sufficient statistics were collected for the calculation of the correlation function a large number of independent samples  $K = 1000$  was used.

Fig. 2 shows the correlation function from the raw data of Fig. 1 and because of the large value of  $K$  it is very smooth. In this plot no averaging of neighbouring points was used to smooth the data (i.e., a binning box size is defined as the number of successive MCS averaged to produce an effective value for the fluctuating quantity). In some runs binning was used to suppress high frequency noise. Maximum binning size used was  $\sim 200$  MCSs. This binning at worst suppresses the very fast time components, i.e., faster by two orders of magnitude than the extracted time constant of the fluctuations. The definition of the autocorrelation function  $C_A(t)$  of a fluctuating quantity  $A(t)$  is

$$C_A(t) = \frac{\langle A(0)A(t) \rangle - \langle A \rangle^2}{\langle A^2 \rangle - \langle A \rangle^2} \quad (5)$$

where  $\langle A \rangle$  is its average value over the time the quantity is monitored. For attractive interaction  $A(t) = S_{\max}/(N\theta)^2$  and for Fig. 2 the extracted time constant is  $\tau_{\text{int}} = 8410$  MCS. The decay time is determined by the time needed for the correlation function to drop to a fixed fraction of its initial value. Since the correlation functions were fitted to exponential functional form,  $\tau$  was taken as the decay constant of the exponential.

Tables 1 and 2 list typical results for attractive interactions and Tables 3 and 4 for repulsive interactions. Table 1 lists the results as a function of coverage for fixed  $J/kT = 2$  and Table 2 lists the results for different ratios  $1.8 < J/kT < 2.2$  at fixed coverage  $\theta = 0.5$ . Table 3 presents similar information for repulsive interactions as a function of coverage and Table 4 as a function of temperature. The first two columns summarize the static information about the average values of the quantities  $S_{\max}$  and  $\langle \Delta S_{\max}^2(0) \rangle^{1/2}$ .  $S_{\max}$  and  $\langle \Delta S_{\max}^2(0) \rangle^{1/2}$  are increasing functions of the average domain size. The mean square deviation  $\langle \Delta S_{\max}^2(0) \rangle^{1/2}$  is a measure of the equilibrium fluctuations of the average domain size (thermodynamically it is proportional to the isothermal compressibility).

The nature of the phase transition is different for the two types of interactions, i.e., for attractive interactions the phase transition is first order (there is coexistence between  $(1 \times 1)$  domains and the empty lattice phase), while for repulsive interactions the phase transition is second order. In both cases one expects that  $S_{\max} = cs^2$  with  $s$  the average diffusion length of the fluctuations. The constant

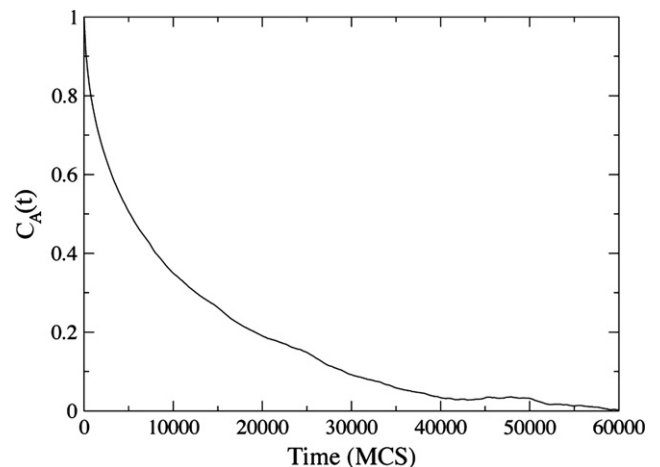


Fig. 2. Correlation function  $C_A(t)$  of the data of Fig. 1 with large value of  $K = 1000$  independent samples used which results in very smooth  $C_A(t)$ . The fluctuating quantity  $A(t)$  is  $S_{\max}/(N\theta)^2$ . The characteristic time  $\tau$  is defined in terms of the decay constant of the exponentially fitted form for  $C_A(t)$  and is used to determine  $D_c$ .

**Table 1**

The dependence of  $S_{\max}$ ,  $\Delta S_{\max}$ ,  $\tau$  and  $D_c/D_0$  on coverage  $\theta$  at fixed  $J/kT = 2$  for the case of attractive interactions

$\theta$	$S_{\max}$	$\Delta S_{\max} = \langle (S_{\max} - \langle S_{\max} \rangle)^2 \rangle^{1/2}$	$\tau$	$D_c/D_0(0)$
0.1	317	144	846	$3.84 \times 10^{-4}$
0.2	1348	374	2264	$1.53 \times 10^{-4}$
0.3	2448	424	3169	$8.82 \times 10^{-5}$
0.4	3087	401	3264	$6.08 \times 10^{-5}$
0.5	3390	454	7137	$1.95 \times 10^{-5}$
0.6	3014	390	6375	$1.35 \times 10^{-5}$
0.7	2390	419	8673	$5.78 \times 10^{-6}$

The ratio  $D_c/D_0$  vs  $\theta$  is graphed in Fig. 3.

**Table 2**

The dependence of  $S_{\max}$ ,  $\Delta S_{\max}$ ,  $\tau$  and  $D_c/D_0$  on  $J/kT$  for  $\theta = 0.5$  and the case of attractive interactions

$J/kT$	$S_{\max}$	$\Delta S_{\max} = \langle (S_{\max} - \langle S_{\max} \rangle)^2 \rangle^{1/2}$	$\tau$	$D_c/D_0(0)$
1.80	2595	527	4129	$2.58 \times 10^{-5}$
1.85	2808	517	5051	$2.28 \times 10^{-5}$
1.90	3017	499	5873	$2.12 \times 10^{-5}$
1.95	3214	481	6491	$2.04 \times 10^{-5}$
2.00	3390	454	7137	$1.95 \times 10^{-5}$
2.05	3544	425	6945	$2.10 \times 10^{-5}$
2.10	3690	400	7174	$2.12 \times 10^{-5}$
2.20	3903	356	8411	$1.91 \times 10^{-5}$

The ratio  $D_c/D_0$  vs  $J/kT$  is graphed in Fig. 4.

**Table 3**

The dependence of  $S_{\max}$ ,  $\Delta S_{\max}$ ,  $\tau$  and  $D_c/D_0$  on coverage  $\theta$  at fixed  $J/kT = -2$  for the case of repulsive interactions

$\theta$	$S_{\max}$	$\Delta S_{\max} = \langle (S_{\max} - \langle S_{\max} \rangle)^2 \rangle^{1/2}$	$\tau$	$D_c/D_0(0)$
0.1	2	2	122	11
0.3	21	19	244	68
0.5	225	190	2501	73
0.7	28	25	13	1671

The ratio  $D_c/D_0$  vs  $\theta$  is graphed in Fig. 5.

**Table 4**

The dependence of  $S_{\max}$ ,  $\Delta S_{\max}$ ,  $\tau$  and  $D_c/D_0$  on  $J/kT$  for  $\theta = 0.5$  and the case of repulsive interactions

$J/kT$	$S_{\max}$	$\Delta S_{\max} = \langle (S_{\max} - \langle S_{\max} \rangle)^2 \rangle^{1/2}$	$\tau$	$D_c/D_0(0)$
1.80	171	136	478	159
1.90	211	168	1136	111
2.00	225	190	2501	73
2.10	236	209	6007	43
2.20	321	222	11066	43

The ratio  $D_c/D_0$  vs  $J/kT$  is graphed in Fig. 6.

$c$  is different for the two cases because the two ordered structures are different (the  $(1 \times 1)$  structure is a dense structure while the  $c(2 \times 2)$  is an open structure) and the diffusion length  $s$  is related differently to the average domain size. The values of  $c$  for the two types of interactions were found empirically by matching the value of  $D_c$  with literature results [19,20] at one point in  $(T, \theta)$ ; the value of  $c$  found from matching at one point was used to deduce  $D_c$  at the other parameter points  $(T, \theta)$  simulated. Since the number of coverages and temperatures simulated is  $\sim 30$  this is a demanding test of the calculated  $D_c$  from the diffraction fluctuation method, whether it has similar coverage and temperature dependence as the other methods.

This empirical identification is in full agreement with the intuitive expectation how the diffusion length  $s$  should be different for the two types of interactions. Also as will be seen shortly the

choice gave very good agreement with the probe area method of calculating  $D_c$  [19,20]. This agreement is non-trivial because the diffraction fluctuation method has not been tested before for  $D_c$  measurements and there is no theory relating the diffusion length  $s$  (during the decay of the fluctuations) to the fluctuations of the superstructure diffracted intensity.

The temperatures chosen in both cases are within the ordered region. For attractive interactions the ordered domains are  $(1 \times 1)$  (with density 1 ML) separated by empty regions (with density 0 ML). The areas covered by the two phases are consistent with the lever's rule so the global coverage is the fixed coverage  $\theta$ . Because of this coexistence a large ordered domain forms close to the maximum size  $(N\theta)$  and therefore  $S_{\max} \approx (N\theta)^2$ . (Because of the small lattice size used  $L = 21$  and the limited wavevector resolution,  $S(q, t)$  has a maximum at  $q_{\max} = (\pi/21, \pi/21)$ , i.e., the wavevector closest to  $q = (0, 0)$ .) The normalization  $c = (N\theta)^2$  implies that the diffusion length  $s = (S_{\max}/c)^{1/2}$  is approximately one lattice constant, since the phase is dense and domain fluctuations are only caused by the motion of perimeter atoms within a few lattice constants.

Tables 3 and 4 show the results for repulsive interactions. Since the order parameter (i.e., the  $c(2 \times 2)$  intensity) is not the concentration and the phase transition is of second order there are larger spatial domain fluctuations. Domains of the ordered  $c(2 \times 2)$  phase are degenerate on the two equivalent sublattices, and the extent of the domains is measured by the intensity at the ordering wavevector  $q_{\max} = (\pi/a, \pi/a)$  (which as described before it is the long wavelength limit for the  $c(2 \times 2)$  phase). The superposition of the intensity from domains on the two different sublattices results in  $S_{\max}$  intensity being proportional to the average domain size. Since the  $c(2 \times 2)$  structure is open and the two equivalent  $c(2 \times 2)$  domains are of comparable size, fluctuations are caused over the whole domain size, and therefore the diffusion length  $s$  which measures the spatial extent of the fluctuations, can be identified by  $S_{\max}^{1/2}$  (as found empirically by choosing  $c = 1$ ).

The difference between the ordering wavevectors (with  $q_{\max}$  being close to  $(0, 0)$ ) for attractive interactions and at  $(\pi/a, \pi/a)$  for repulsive interactions explains the difference in the magnitude of  $S_{\max}$  for the two cases.  $S_{\max}$  is approximately an order of magnitude larger for attractive than for repulsive interactions. Correspondingly the increase of the relative spatial fluctuations for the two cases is also seen from the ratio  $\langle \Delta S_{\max}^2(0) \rangle^{1/2}/S_{\max}$  which is bigger by a factor of  $\sim 10$  for repulsive interactions because larger fluctuations are expected for second order phase transitions. Although the lattice size used is  $21 \times 21$  and relative fluctuations are larger for the case of repulsive interactions, this does not affect the extracted quantities (the time constant  $\tau$  and the value of  $S_{\max}$ ) since all the parameters used of coverage  $\theta$  and temperature  $T$  were not in the critical region where diverging fluctuations become more important. Since our goal was to determine  $D_c$  which is sensitive to coverage fluctuations and not order parameter fluctuations it would have no strong singular dependence even if we probe the critical region (for much larger lattice sizes).

The relation between  $S_{\max}$  and  $s$  defines the absolute value of the collective diffusion coefficient extracted from the diffraction fluctuation method  $D_c = s^2/4\tau$  since the measured diffraction fluctuations are the ones caused by mass transport over a distance  $s$ . The exact relation between  $S_{\max}$  and  $s$  affects the prefactor of  $D_c$ , but because of the earlier discussion about the empirically found relation between  $S_{\max}$  and  $s$ , the prefactor is fully determined from the deduced values of  $c$ . Using the value for a single atom  $D_c(\theta \rightarrow 0) = v_{\max}/4$  we can rewrite the diffusion coefficients as ratios  $D_c/D_c(0) = S_{\max}/(N\theta)^2\tau$  for attractive interactions (since  $v_{\max} = 1$  in this case) and  $D_c/D_c(0) = e^{3J/kT}S_{\max}/\tau$  (since  $v_{\max} = e^{3J/kT}$ ). A different way of interpreting  $v_{\max}$  is in terms of the inverse of the time interval  $\Delta t = v_{\max}^{-1}$  corresponding to 1 MCS, i.e.,  $v_{\max}$  is the

normalization of the probabilities for each of the possible nearest neighbour jumps of a diffusing atom to ensure that is less than one.

The relation between  $S_{\max}$  and  $s$  for the two cases should be valid even for domain fractal like morphology, which is the case for both type of interactions (but more pronounced for attractive interactions).

Fig. 3 shows  $D_c$  vs  $\theta$  for  $J/kT=2$  (which corresponds to  $T/T_c=0.88$ ). It follows a monotonic decay with  $\theta$  as observed in [20]. The  $D_c/D_c(0)$  vs  $\theta$  changes from  $2 \times 10^{-3}$  to  $9 \times 10^{-4}$  as  $\theta$  changes from 0.1 to 0.7 ML. The coverage trend is similar to the one in [20] for the lowest temperature used  $T/T_c=0.95$ . It is remarkable that not only  $D_c$  decreases with  $\theta$ , as expected for attractive interactions, but also the absolute value of  $D_c$  is in excellent agreement with the choice  $c=(N\theta)^2$ . Since the relation between  $S_{\max}$  vs  $s$  is empirical and although heuristically justified in terms of the different topology of the two phases, a more rigorous justification is needed. The values of  $\tau$  and the ratio  $D_c/D_c(0)$  are also shown in Table 1. There is an increase in  $\tau$  by a factor of 10 with  $\theta$  (which is a result of the increasing number of nearest neighbour bonds with  $\theta$ ) that increases the local diffusion barrier. This increase of  $\tau$  with coverage would have been sufficient to prove the applicability of the diffraction fluctuation method, but the good agreement with the absolute values of [20] is even stronger evidence.

Fig. 4 shows the Arrhenius plot for the ratio  $D_c/D_c(0)$  vs  $J/kT$  at constant  $\theta=0.5$  to be compared with the results of Fig. 9 of [20] although their temperature range was higher  $0 < J/kT < 1.75$  than the one used in the current work. The data in [20] were fitted to two Arrhenius plots and all of the temperatures were in the disordered region. The activation energy in Fig. 4 is rather low when compared with the one in [20], which found an increase of the activation energy in the lower temperature branch. Possibly the reason why  $D_c/D_c(0)$  becomes temperature independent in the diffraction fluctuation method, is because the fluctuations originate from isolated diffusion of monomers over few lattice constants as are exchanged between domains (over the lower temperature range in the current work  $0.72 < T/T_c < 0.98$ ). Free monomers have no nearest neighbour bonds and the diffusion barrier should be temperature independent.

Fig. 5 shows  $D_c/D_c(0)$  vs  $\theta$  for  $J/kT=-2$ , the case of repulsive interactions. Again the increasing trend with coverage seen in the previous work [19] is also found with the current simulations. The agreement is even better for the absolute value of  $D_c$  with [19] based on the identification of the constant  $c=1$ .

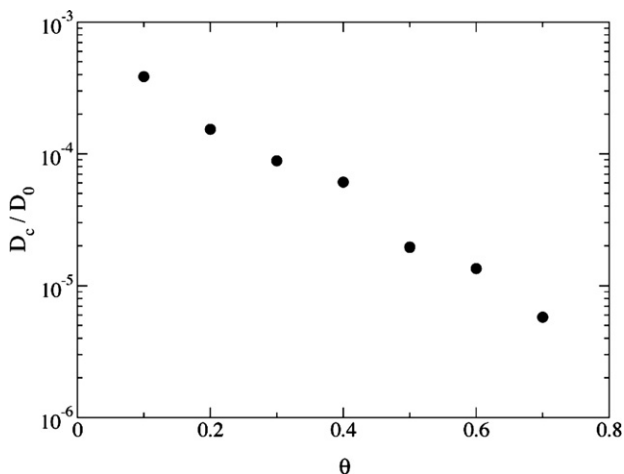


Fig. 3.  $D_c/D_c(0)$  vs  $\theta$  for  $J/kT=2$  (attractive interactions) which follows a monotonic decay as  $\theta$  is changed with good agreement with Ref. [20].  $D_0$  denotes  $D_c(\theta=0)$ .

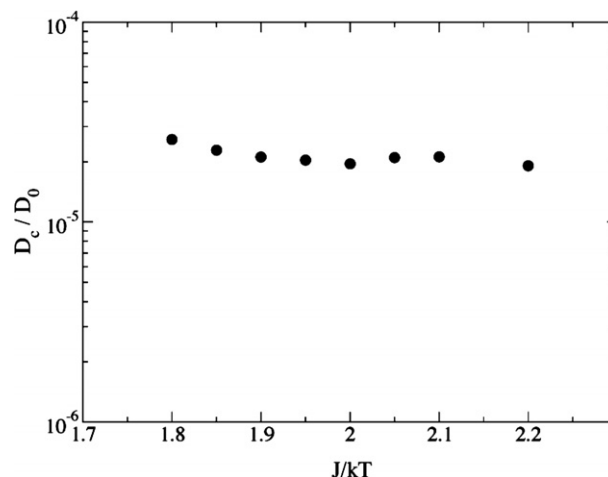


Fig. 4. Arrhenius plot for the ratio  $D_c/D_c(0)$  vs  $J/kT$  at constant  $\theta=0.5$  for attractive interactions. The effective activation energy is close to zero.  $D_0$  denotes  $D_c(\theta=0)$ .

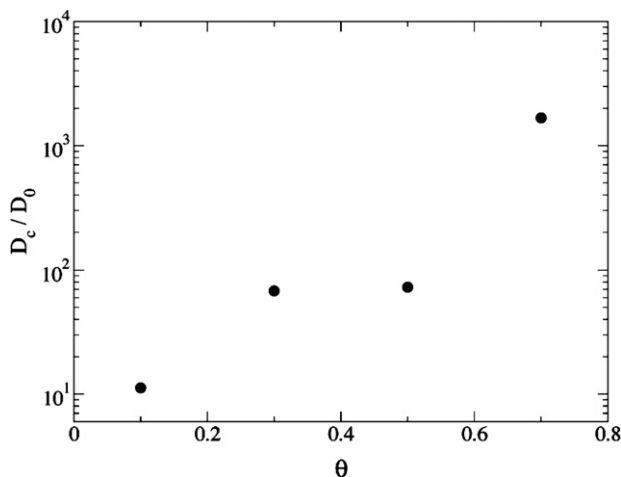
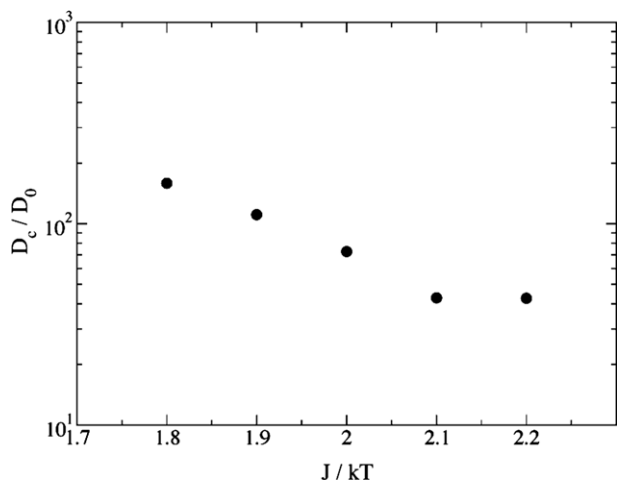


Fig. 5.  $D_c/D_c(0)$  vs  $\theta$  for  $J/kT=-2$  for  $\theta=0.5$  ML (and for repulsive interactions). The increasing trend with  $\theta$  and the absolute values of  $D_c/D_c(0)$  are in good agreement with Ref. [19].  $D_0$  denotes  $D_c(\theta=0)$ .

$D_c/D_c(0)$  increases from 6 to close to 830 as  $\theta$  changes from 0.1 to 0.7 ML. The corresponding variation at the closest temperature used by [19]  $J/kT=-1.76$  (while in Fig. 5 is  $J/kT=-2$ ) is from 2 to 300 as  $\theta$  changes from 0.1 to 0.9 ML, which is in excellent agreement.

Fig. 6 shows the Arrhenius plot of  $D_c/D_c(0)$  vs  $J/kT$  for fixed  $\theta=0.5$  ML in the ordered region.  $D_c$  decreases with decreasing  $T$  and the effective activation energy is positive. It is approximately  $E=1.55$  J. The corresponding data from [19] which were taken mostly in the disordered region have a decreasing  $D_c$  with increasing  $T$  which implies that the activation energy is negative as expected for repulsive interactions. Only in the range  $-1.7 > J/kT > -2.4$  when the system enters the ordered phase (as in the current simulations)  $D_c$  decreases with decreasing  $T$  and an effective fit to Arrhenius dependence results in a positive activation energy of 1.8 J consistent with the activation energy of Fig. 6. The reason for this is that when the system is in the ordered region and  $c(2 \times 2)$  domains form, atoms do not feel the effect of the repulsive interactions because  $c(2 \times 2)$  is an open structure. All four neighbouring sites are vacant and the repulsive energy has no contributions to the barrier which also justifies why the diffusion length  $s$  becomes comparable to the domain size.



**Fig. 6.** Arrhenius plot of  $D_c/D_0$  vs  $J/kT$  for  $\theta = 0.5$  ML.  $D_c/D_0$  decreases with decreasing  $T$  and the effective activation energy is positive. It is  $E = 1.55$  J.  $D_0$  denotes  $D_c(\theta = 0)$ .

## 5. Discussion

These preliminary simulation results using diffraction intensity fluctuations to measure time-dependent correlation functions for  $D_c$  are very promising because of the good agreement with the results from the probe area method, after  $D_c$  is matched at one point in  $T, \theta$  parameter space. Both the coverage and temperature dependence are in good agreement for all runs; except the case of lower activation energy for attractive interactions. This can be an indication that the fluctuations are caused by monomer diffusion between the dense ( $1 \times 1$ ) domains (the diffusion barrier is not affected by the interactions since the monomers have zero number of bonds). One of the advantages of the diffraction fluctuation method is that it is ideally suited for studies of dynamic phenomena and diffusion measurements at low temperatures within the ordered region of the phase diagram.

This comparison is better seen in Figs. 7–10 where we plot the results of this work with the results of Refs. [19,20] over the whole temperature and coverage range explored. In this comparison we include all the different ways used in [19,20] to probe the equilib-

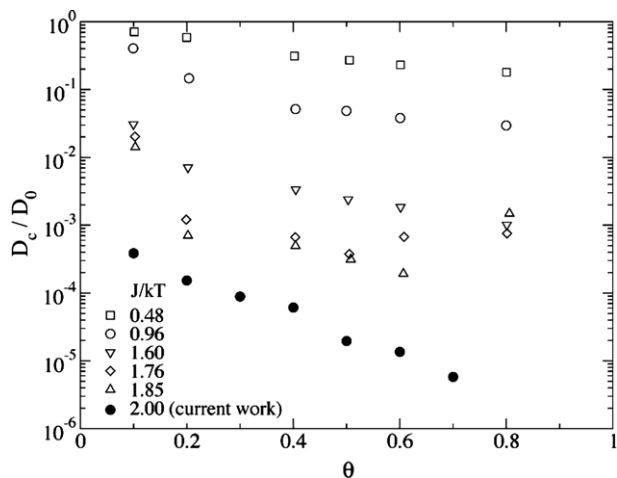


**Fig. 7.**  $D_c/D_0$  vs  $\theta$  for different attractive interactions listed from Ref. [20] and the results of the current work. Excellent agreement both on the dependence on  $\theta$  and the absolute values of  $D_c/D_0$  between the different calculations.  $D_0$  denotes  $D_c(\theta = 0)$ .

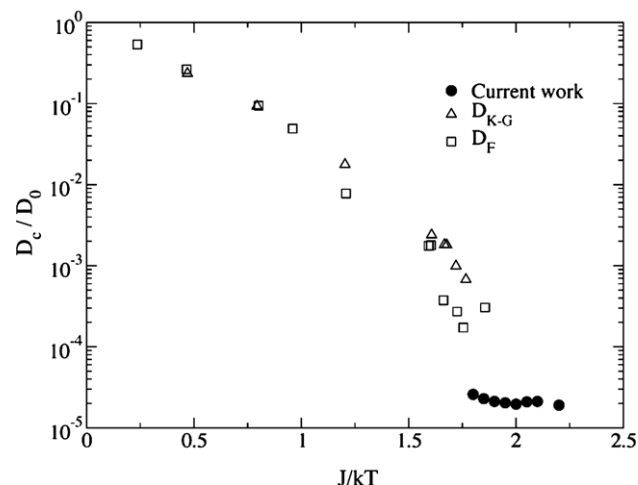


**Fig. 8.**  $D_c/D_0$  vs  $J/kT$  between the results of [20] with two different methods (Kubo-Green and probe area fluctuation method) and  $\theta = 0.5$  ML with the results of the current method. It is seen that the current method is ideally applicable within the ordered region and the results fit as an extrapolation of the results obtained from conventional methods.  $D_0$  denotes  $D_c(\theta = 0)$ .

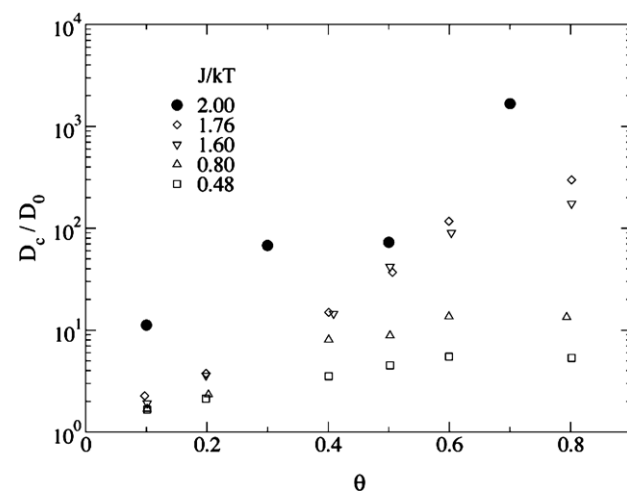


**Fig. 9.**  $D_c/D_0$  vs  $\theta$  for different type of repulsive interactions listed from Ref. [19] and the results of the current work. Excellent agreement both on the dependence on  $\theta$  and the absolute values of  $D_c/D_0$  between the different calculations.  $D_0$  denotes  $D_c(\theta = 0)$ .

rium relaxation of an interactive system and extract the corresponding diffusion coefficients. Figs. 7 and 8 show the results for attractive and Figs. 9 and 10 repulsive interactions. These plots illustrate first the different temperature range of the current method, since it is suited within the ordered region for both types of interactions while the results of [19,20] were mainly in the disordered region with some overlap between the sets. In [19,20] different ways to measure collective diffusion were used, i.e., the fluctuation method based on a probe area, the chemical diffusion coefficient (which is equivalent to the Kubo-Green diffusion coefficient) and the jump-rate diffusion coefficient defined by

$$D_c \left( \frac{1}{4t} \right) \left( \frac{\partial(\mu/kT)}{\partial \ln \theta} \right)^{-1} \left\langle \left( \frac{1}{N} \sum_i \Delta r_i \right)^2 \right\rangle = \left( \frac{\partial(\mu/kT)}{\partial \ln \theta} \right)^{-1} D_J \quad (6)$$

where  $t$  is the time,  $\Delta r_i = \Delta x_i \hat{x} + \Delta y_i \hat{y}$  is the displacement of the  $i$ th atom,  $\mu$  is the chemical potential and  $N$  is the number of atoms in

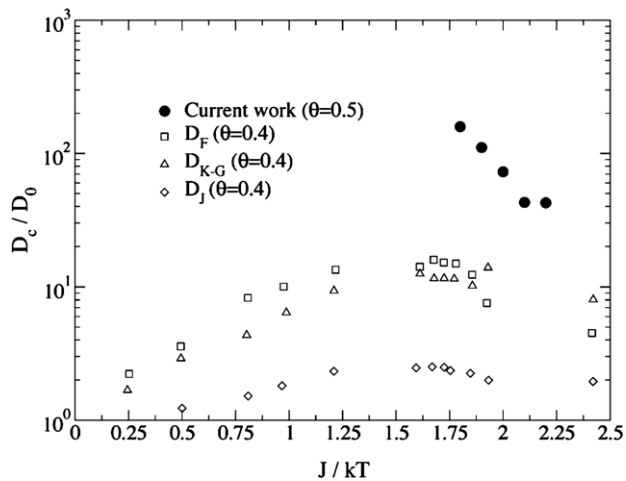


**Fig. 10.**  $D_c/D_0$  vs  $J/kT$  between the results of [19] with three different methods (Kubo–Green, probe area fluctuation and jump-rate diffusion coefficients) and  $\theta = 0.4$  ML (close to the coverage of the current work  $\theta = 0.5$  ML because this coverage is not available in [19]). It is seen that the current method is ideally applicable within the ordered region.  $D_0$  denotes  $D_c(\theta = 0)$ .

the system. All three methods are shown in the temperature dependent plots. For the coverage dependence only  $D_c$  is shown from [19,20] at fixed  $J/kT$ .

These plots not only show the wide range of  $(T, \theta)$  parameter space probed, but also more importantly show that the results of the diffraction fluctuation method can be thought as natural extrapolation of the high temperature results obtained, with the conventional methods. This is a very concise and illustrative way to demonstrate the legitimacy of the new method.

However, despite the optimal use of the method for the ordered region, it is possible to extend the method in the disordered region of the phase diagram, i.e., above the transition temperature  $T_c$ . In this case there is no sharp peak at the ordering wavevector, because long range order is absent. But the short range order still leads to a weaker maximum at a characteristic wavevector (defined by the average distance between neighbouring atoms). The diffusive motion of the atoms will cause fluctuations of the intensity. Collecting signal for sufficiently long time at this characteristic wavevector can recover the time constant of the diffusive motion. Under other experimental conditions than the formation of domains of the ordered phases, fluctuations can be caused by the motion of a very small amount of foreign atoms in disordered positions (which do not generate a superstructure spot) but can have very different scattering factors. Such experiments are possible with He-scattering even at low coverages, since it is known that large scattering cross sections are possible with He-scattering (several times their geometric size) and therefore larger contrast between substrate and foreign atoms.

The form of the correlation functions found in the models of the current studies was fitted to an exponential functional form which was a strong indication that memory effects can be neglected. Testing the functional form of the correlation functions close to second order phase transition and especially whether the diffusive tail  $1/t$  is present or modified according to long wavelength relaxations within the critical region (typical of 2-d diffusion[21,22]) might require runs on larger sizes. The goal is to distinguish the functional form. This possibility will allow the measurement of dynamic critical phenomena especially close to phase transitions.

Previous work [23–25] has utilized the  $S_{\max}$  vs  $t$  during non-equilibrium domain growth kinetics to extract a non-equilibrium time-dependent  $D_c$  which with time evolves towards its expected

value at equilibrium. In the previous work on several models it was shown that although  $D_c$  becomes time-dependent its behaviour can be fully understood in terms of how the atoms are distributed between sites of different binding. This should be expected also in the current method since depending on the extent of how far the system is from equilibrium and the domains have smaller sizes, more atoms will be at sites of reduced binding and therefore larger diffusion coefficient should be expected. The current work extends naturally this analysis using the dynamic structure factor  $S(q, t)$  after growth is completed, because it demonstrates that once equilibrium is established the  $D_c$  is also measurable from equilibrium fluctuations of  $S_{\max}$  vs  $t$ .

## 6. Summary

The study of equilibrium collective diffusion coefficients in the long wavelength approximation requires measurements of the autocorrelation of the concentration fluctuations. A recently proposed experimental method [14–16] is based on using the equilibrium structure factor  $S(q, t)$  which is routinely measured in diffraction experiments. The goal of the present work was to test if this method is also applicable to collective diffusion measurements in systems with interactions. It was shown that indeed the collective diffusion coefficient can be measured from the decay constant of the fluctuations. With Monte Carlo simulations we tested this method on models with nearest neighbour attractive and repulsive interactions because different dependence on coverage is expected, so this provides good testing of the method. A monotonically decreasing  $D_c$  is found for attractive and monotonically increasing  $D_c$  with  $\theta$  is found for the case of repulsive interactions. Furthermore, the absolute value of  $D_c$  is in excellent agreement with the one deduced from the probe area correlation function once the values of  $D_c$  at one point in  $(T, \theta)$  space are matched. This demonstrates the value of the novel method in measuring equilibrium dynamic phenomena although further work is needed to justify the method in other model systems and analytically.

## Acknowledgment

Work at the Ames Laboratory was supported by the Department of Energy-Basic Sciences under Contract DE-AC02\_07CH11358. This work was supported by the Director for Energy Research Office of Basic Energy Sciences. The project was also funded from the Greek Secretariat of Research and Technology in the frame of Bilateral Agreements between Greece and USA.

## References

- [1] M.C. Tringides (Ed.), Surface Diffusion: Atomistic and Collective Processes, Plenum, New York, 1997.
- [2] M.C. Tringides, Z. Chvoj (Eds.), Collective Diffusion on Surfaces: Correlation Effects and Ad atom Interactions, Kluwer, 2001.
- [3] Z. Chvoj, J. Phys. Condens. Matter. 12 (2000) 2135.
- [4] J.M. Lahtinen, M. Mašín, T. Laurila, T. Ala-Nissila, Z. Chvoj, J. Chem. Phys. 116 (2002) 7666.
- [5] A. Danani, R. Ferrando, E. Scalas, M. Torri, Int. J. Mod. Phys. B 11 (1997) 2217.
- [6] T. Ala-Nissila, R. Ferrando, S.C. Ying, Adv. Phys. 51 (2002) 949.
- [7] M.A. Zaluska-Kotur, Z.W. Gortel, Phys. Rev. B 74 (2006) 045405.
- [8] M.C. Tringides, R. Gomer, Surf. Sci. 265 (1992) 283.
- [9] R. Gomer, Surf. Sci. 38 (1973) 373.
- [10] M.C. Tringides, M. Gupalo, Q. Li, X. Wang, Proceedings of XI Max Born Symposium, in: R. Kutner, A. Pelkalski (Eds.), Springer-Verlag, 1998.
- [11] M.L. Lozano, M.C. Tringides, Europhys. Lett. 30 (1995) 537.
- [12] X. Xiao, X.D. Zhu, W. Daum, Y.R. Shen, Phys. Rev. Lett. 61 (1988) 2883.
- [13] J.W. Frenken, B.J. Hinch, J.P. Toennies, Ch. Woll, Phys. Rev. B 41 (1990) 938.
- [14] Z. Chvoj, E.H. Conrad, M.C. Tringides, Phys. Rev. B 15 62 (2000) 4672.
- [15] E.H. Conrad, A. Menzel, S. Kiriukhin, M.C. Tringides, Phys. Rev. Lett. 81 (1998) 3175.
- [16] M. Kammler, M. Horn Von Hogen, N. Voss, M.C. Tringides, A. Menzel, E.H. Conrad, Phys. Rev. B 65 (2002) 075312.

- [17] S. Brauer, G.B. Stephenson, M. Sutton, R. Bruning, E. Dufresne, S.G.J. Mochrie, G. Grubel, J. Als-Nielsen, D.L. Abernathy, *Phys. Rev. Lett.* 74 (1995) 2010.
- [18] R. Gomer, *Rep. Prog. Phys.* 53 (1990) 917.
- [19] C. Uebing, R. Gomer, *J. Chem. Phys.* 95 (10) (1991) 7626.
- [20] C. Uebing, R. Gomer, *J. Chem. Phys.* 95 (10) (1991) 7636.
- [21] Q. Li, M.C. Tringides, *Surf. Sci.* 365 (1996) 495.
- [22] X. Wang, Q. Li, M.C. Tringides, *Phys. Rev. B* 57 (1998) 7275.
- [23] E. Arapaki, P. Argyrakis, M.C. Tringides, *Phys. Rev. B* 62 (2000) 8286.
- [24] I. Vattulainen, J. Merikoski, T. Ala-Nisila, S. Ying, *Surf. Sci.* 366 (1996) L697.
- [25] Z. Chvoj, *Surf. Sci.* 507–510 (2002) 114.